Leveraging Deep-Learning for Adaptive Coding and Modulation for LEO Satellite-Terrestrial Networks

Yuhan Xia*, Xin Zhang*, Xiaohan Qin*, Zitian Zhang†, Yu Zhang‡, Ting Ma§, Haibo Zhou*
*School of Electronic Science and Engineering, Nanjing University, Nanjing, China, 210023
†School of Information and Electronic Engineering, Zhejiang Gongshang University, Hangzhou, China, 310018
‡Topxgun Robotics Co., Ltd, Nanjing, China, 211100
§School of Electronic and Optical Engineering, Nanjing University Of Science and Technology, Nanjing, China, 210094
Email: yuhanxia@smail.nju.edu.cn, zanxin@smail.nju.edu.cn, xhderemail@smail.nju.edu.cn,
zitian.zhang@mail.zjgsu.edu.cn, yzhang@topxgun.com, tingma@njust.edu.cn, haibozhou@nju.edu.cn

2024 IEEE/CIC International Conference on Communications in China (ICCC) | 979-8-3503-7841-2/24/$31.00 ©2024 IEEE | DOI: 10.1109/ICCC62479.2024.10681710

***Abstract*—Low-earth-orbit (LEO) satellite-terrestrial network (LSTN) is expected to play a significant role in the next-generation wireless networks (6G), providing global coverage and facilitating various 6G applications. However, the high dynamics of channel state information (CSI) in LSTN have posed challenges to modulation and coding schemes (MCS), which adversely affects the correctness of data transmission and the quality of service (QoS) expected by users. To enhance the communication reliability of LSTN, in this paper, we investigate the adaptive coding and modulation (ACM) method under the digital video broadcasting (DVB) standards. We first establish a channel model and then introduce an ACM method involving channel state estimation, channel state prediction, and MCS switching. Subsequently, the least squares (LS) algorithm is leveraged for channel estimation and we propose an ARIMA-Bidirectional Long Short-Term Memory (AB-LSTM) algorithm specifically for forecasting time-series signal-to-noise ratio (SNR) values for precise channel prediction. Then MCS switching is conducted based on the predicted SNR and switching threshold based on DVB standards. We conduct extensive simulations to show that our proposed algorithms can achieve higher estimation and prediction accuracy, and the introduced ACM method can effectively optimize the usage of channel capacity.**

***Index Terms*—LEO satellite-terrestrial network, adaptive coding and modulation, DVB, modulation and coding scheme.**

I. Introduction

Currently, the low-earth-orbit (LEO) satellite-terrestrial network (LSTN), which significantly enhanced the data transmission capacity of terrestrial networks, is expected to become a crucial component of the next-generation wireless networks (6G) [1]. Furthermore, the emergence of ultra-dense LEO constellations, such as SpaceX and OneWeb, has the potential to provide global communication coverage, significantly accelerating the development of various technologies, including internet-of-things (IoT) technologies, remote surgery, and vehicle-to-everything (V2X) communication [2], [3]. However, the high dynamics of LEO satellites introduces variations in the quality of service (QoS) for LSTN users, necessitating the design of more flexible communication protocols and algorithms to ensure the stability and reliability of data transmission. Currently, the digital video broadcasting (DVB) physical layer standards, which include both constant coding and modulation (CCM) and adaptive coding and modulation (ACM) methods are utilized by Starlink [4]. Traditional CCM methods in LSTNs are typically designed conservatively to accommodate the worst channel conditions, leading to suboptimal utilization of spectral resources. Consequently, the ACM method, which enables real-time modulation and coding scheme (MCS) switching based on the detection of varying channel states, is of critical significance.

Due to their lower orbital altitude, LEO satellites move quickly relative to the Earth's surface, which results in rapidly changing channel conditions, posing challenges for the real-time adjustment of MCS in the ACM method [5]. To effectively address this issue, it is essential to acquire accurate channel state information (CSI) and ensure that the communication system updates the CSI rapidly and frequently. Xu *et al*. [6] designed a vector algorithm based on sparse Bayesian learning, which achieves better channel estimation performance and more flexible device activity. Ji *et al*. [7] proposed an ACM method utilizing convolutional neural networks (CNNs) that extracts features related to channel and noise estimation from the receiver. Subsequently, the transmitter adjusts its modulation strategy accordingly to optimize communication quality. However, previous studies on ACM methods in LSTNs primarily focused on static LEO satellites [8] or only considered satellite channel state estimation [9], ignoring the CSI obsolescence that can result from the time-varying nature of satellites and channels. Implementing dynamic channel modeling and channel state prediction can effectively address this issue.

Inspired by the considerations mentioned above, we investigate the ACM method in dynamic LSTN based on DVB physical layer standards. Our goal is to enable the system to perform precise channel state estimation and prediction under rapidly changing conditions, and promptly switch MCSs while maintaining the reliability of the communication link. The primary contributions of this paper are summarized as follows:

- We develop an ACM method based on the DVB standards which includes channel state estimation, channel state prediction, and MCS switching, taking into account the mobility of LEO satellites and the dynamic nature of the satellite-to-ground channels.
- We use the least squares (LS) algorithm for channel estimation and design an algorithm that combines an au-

toregressive integrated moving average (ARIMA) model with a bidirectional long short-term memory (BiLSTM) neural network to accurately predict channel state.
- We conduct simulation comparisons between our proposed algorithms and the baseline algorithms. The results indicate that our algorithms have smaller errors, and the ACM method we proposed can adjust the MCS in real time based on channel variations.

The rest of this paper is structured as follows. Section II describes the establishment of the LSTN model, and presents the specific approach to the ACM method. Section III introduces the algorithm designed for channel state prediction. Section IV evaluates the performance of channel state estimation and channel state prediction algorithms compared with baselines. Section V is the conclusion.

II. System Model

The LSTN communication scenario is illustrated in Fig. 1. In this section, we establish a channel model that accounts for free space path loss, ground object loss, rain attenuation, cloud attenuation, and gas attenuation. Additionally, we propose an ACM method based on the DVB-satellite-second generation extension (DVB-S2X) physical layer standard [10].

A. Scenario Description

For a single LEO satellite, the distance d from the ground station to the satellite can be expressed as:

$$d = \sqrt{R_e^2 + (R_e + h)^2 - 2R_e(R_e + h)\cos\psi}, \tag{1}$$

where R_e is the radius of the Earth, h is the altitude of the satellite orbit, and ψ is the central angle. The elevation angle θ is the angle from the ground station's line of sight upward to the satellite, which can be calculated as:

$$\theta = 90^\circ - \alpha - \psi, \tag{2}$$

where α is the angle observed from the ground station to the satellite through the center of the Earth, which can be calculated using the cosine theorem:

$$\alpha = \cos^{-1}\left(\frac{R_e\cos\psi - (R_e + h)}{d}\right). \tag{3}$$

B. Channel Model

Following International Telecommunication Union (ITU) standards, we conduct channel modeling using a 30 GHz carrier, considering factors such as free space path loss, ground object loss, rain attenuation, cloud attenuation, and gas attenuation. Below, we introduce these various influencing factors:

1) Free Space Path Loss

The free space path loss L_f between a LEO satellite and a ground station which describes the energy loss of electromagnetic waves as they propagate through the vacuum or ideal free space can be expressed as:

$$L_f = 32.45 + 20\log_{10}(f) + 20\log_{10}(d), \tag{4}$$

where f is the carrier frequency, and d is the distance between the ground station and the LEO satellite.

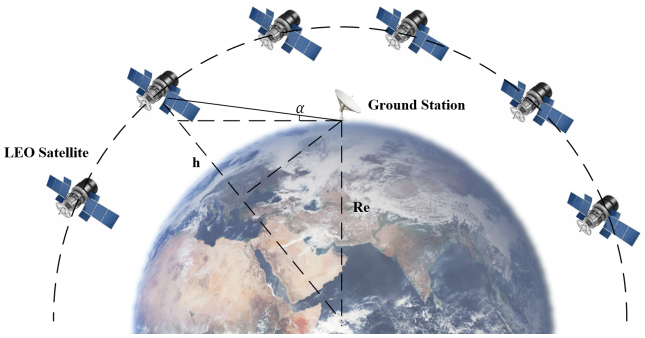

Fig. 1. LSTN communication scenario.

2) Ground Object Loss

We adopt the ground object loss calculation method suitable for urban and suburban environments, as recommended by ITU-R P.2108 [11]. The specific calculation formula is:

$$L_o = \{-93f^{0.175}\left[\ln\left(1 - \frac{p'}{100}\right)\right]\cdot\cot\left[0.05\left(1 - \frac{\alpha}{90}\right) + \frac{\pi\alpha}{180}\right]\} - 1 - 0.6Q^{-1}\left(\frac{p'}{100}\right), \tag{5}$$

where Q^{-1} is the inverse complementary normal distribution function, and p' describes the probability that the ground object loss at the ground station is less than the loss calculated by the above formula.

3) Rain Attenuation

We calculate the rain attenuation caused by raindrops on satellite signal propagation according to ITU-R P.618 [12] as follows:

$$L_a = K(R_{0.01})^\beta L_E, \tag{6}$$

where $R_{0.01}$ represents the probability that the annual average rainfall exceeds 0.01%. K and β are constants that can be obtained from ITU standards, and L_E is the effective path length.

4) Cloud Attenuation

According to ITU-R P.840 [13], taking into account the physical properties of clouds, cloud attenuation $L_c(dB/km)$ is modeled as:

$$L_c = K_c(f, T)\rho_c, \tag{7}$$

where K_c is the specific attenuation coefficient of liquid water in clouds (g/m^3), ρ_c is the liquid water density in clouds or fog (g/m^3) and T is the temperature of the liquid water in clouds.

5) Gas Attenuation

Gas attenuation refers to the reduction in the intensity of electromagnetic signals as they propagate through the atmosphere. According to ITU-R P.676 [14], the gas attenuation for signal over 30GHz can be represented as follows:

$$L_g = \left[\frac{7.2r_t^{2.8}}{f^2 + 0.34r_p^2 r_t^{1.6}} + \frac{0.62\zeta_3}{(54 - f)^{1.16}\zeta_1 + 0.83\zeta_2}\right]\cdot\left(f^2 r_p^2 \times 10^{-3}\right), \tag{8}$$

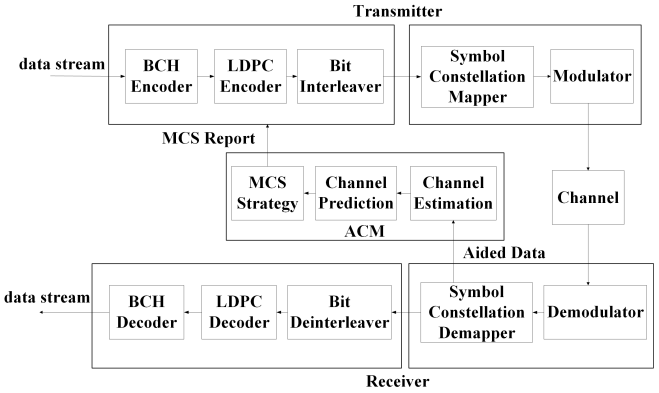

Fig. 2. DVB-S2X physical layer mechanism.

where $r_p = p/1013$, p is the pressure in hPa, and $r_t = 288/(273 + T')$, T' is the temperature in degrees Celsius. The value of ζ can be obtained from the recommendation document.

C. ACM in LSTN

ACM technology is widely utilized to improve bandwidth and power efficiency in communication systems with limited bandwidth and power. Additionally, the ACM method is implemented by continuously monitoring the quality of the channel, such as CSI and SNR, and selecting the appropriate MCS based on changes in the channel conditions. Under favorable channel conditions, higher-order modulation schemes and reduced coding redundancy are employed to enhance the data transmission rate and maximize channel capacity utilization. Conversely, when channel conditions degrade, lower-order modulation schemes and increased coding redundancy are utilized to maintain transmission reliability.

We employ the DVB-S2X physical layer standard, which is currently widely used for broadcasting, professional video transmission, and broadband satellite access. In the DVB-S2X standard, Bose–Chaudhuri–Hocquenghem (BCH) outer codes and low-density parity-check (LDPC) inner codes are used as forward error correction (FEC) channel coding techniques, with code rates including 1/4, 1/3, 2/5, etc. As can be seen in Fig. 2, on the transmitter side, after coding and interleaving, symbol mapping and modulation are carried out, including BPSK, QPSK, 8APSK, etc. The signal then passes through the satellite channel, and on the receiver side, demodulation and decoding processes are performed. Within this framework, the ACM method handles channel state estimation, channel state prediction, and MCS switching. The specific processes are as follows:

1) Conduct physical layer simulations according to the DVB-S2X standard and then generate bit error rate (BER) curves relative to SNR for the selected 42 types of MCS. We set the BER at the switching point to 10^{-3}, and determine the SNR threshold for each MCS at this switching point.
2) Insert pilot signals into the transmitted signals, which pass through the satellite-to-ground communication channel. After receiving the signals, the receiver extracts the pilot signals. The extracted pilot signals are used for SNR estimation.
3) The receiver predicts the SNR for the next moment based on the estimated SNR values. The predicted SNR values are input into the MCS switching table to find the next moment's channel quality indication (CQI) index, and this information is then transmitted back to the transmitter.
4) Upon receiving this CQI index, the transmitter can switch the MCS for transmitting data in the next moment.

III. Algorithm Design

In this section, we specifically introduce the key technologies in the ACM method, including channel state estimation, channel state prediction, and MCS switching strategy.

A. Channel State Estimation

We use the least squares (LS) estimation method, which has been proven to have good estimation performance. The LS estimator estimates the channel by minimizing the sum of the squared errors between the received signals and the signals transmitted through the channel. Assuming that the pilot signal from the transmitter is $x = (x_1, x_2, ..., x_n)$, the received signal can be expressed as the sum of the transmitted signal x affected by the channel H and noise n, that is:

$$y = Hx + n. \tag{9}$$

If there are multiple pilot signals, construct the observation matrix X, with each row corresponding to a pilot signal. Using the LS method, the channel is estimated by minimizing the sum of the squares of the errors. The error e can be defined as follows:

$$e = y - XH, \tag{10}$$

then minimizing the sum of squares of e yields the expression for the channel estimate $\hat{h}$, which is:

$$\hat{H} = (X^T X)^{-1} X^T y, \tag{11}$$

after obtaining the channel estimation, calculate the signal power and noise power as follows:

$$P_{\text{signal}} = |\hat{H}x|^2, \tag{12}$$

$$P_{\text{noise}} = |y - \hat{H}x|^2. \tag{13}$$

The SNR obtained from the LS estimation algorithm can be expressed as follows:

$$\gamma = \frac{P_{\text{signal}}}{P_{\text{noise}}} = \frac{\left|(X^T X)^{-1} X^T y \cdot x\right|^2}{\left|y - (X^T X)^{-1} X^T y \cdot x\right|^2}. \tag{14}$$

Algorithm 1 Time series forecasting algorithm combining ARIMA and BiLSTM (AB-LSTM).

Input: Time based SNR sequence $(\gamma_{k-l}, \gamma_{k-l+1}, ..., \gamma_k)$, length of the sequence l, prediction step n.

Output: Predicted SNR $\hat{\gamma}_{k+n}$.

1: Set initial time k.
2: **repeat**
3: Input $(\gamma_{k-l}, \gamma_{k-l+1}, ..., \gamma_k)$ into ARIMA(p, m, q) to obtain n step prediction values $(\hat{\gamma}_{k-n}, \hat{\gamma}_{k-n+1}, ..., \hat{\gamma}_k)$.
4: Obtain the residual series $(e_{k-n+1}, e_{k-n+2}, ..., e_k)$ by subtracting the predicted SNR series from the input SNR series.
5: Use the residual sequence $(e_{k-n+1}, e_{k-n+2}, ..., e_k)$ as the input of BiLSTM to predict the residual error for the subsequent time step, $\hat{e}_{k+1}$.
6: Update p, q;
7: **until** the minimum predicted residual corresponding to p_k and q_k is obtained.
8: Feed the SNR sequence $(\gamma_{k-l}, \gamma_{k-l+1}, ..., \gamma_k)$ into ARIMA(p_k, m, q_k) to derive the n step forecasted value of SNR $\hat{\gamma}_{k+n}$.
9: Return $\hat{\gamma}_{k+n}$.

B. Channel State Prediction

We propose a deep learning-based channel state prediction algorithm, AB-LSTM, which combines ARIMA with the BiLSTM neural network.

ARIMA is a statistical model used for time series analysis and forecasting, which combines autoregression (AR), differencing (I), and moving average (MA) methods to handle different types of time series data. The basic idea of the ARIMA algorithm is to transform a non-stationary series into a stationary one by differencing the time series data, and then to model and predict the stationary series using autoregressive and moving average methods [8].

The AR component captures the linear relationship between current and past values, representing autocorrelation within the time series. The mathematical expression is:

$$y_t = \phi_1 y_{t-1} + \phi_2 y_{t-2} + \ldots + \phi_p y_{t-p} + \varepsilon_t, \tag{15}$$

where y_t is the current value of the time series, $\phi_1, \phi_2, ..., \phi_p$ are the model parameters, p is the order of autoregression, and ε_t is the white noise error term.

The I part transforms a non-stationary series into a stationary one by calculating the differences between adjacent data points in a sequence of values, which can be typically represented as:

$$y_t' = y_t - y_{t-1}. \tag{16}$$

For non-stationary series, it may be necessary to perform multiple differencings until the series becomes stationary, with m typically representing the order of differencing.

The MA part describes the relationship between the current value and past error terms, which can be expressed as:

$$y_t = \varepsilon_t + \theta_1 \varepsilon_{t-1} + \theta_2 \varepsilon_{t-2} + \ldots + \theta_q \varepsilon_{t-q}. \tag{17}$$

where $\theta_1, \theta_2, ..., \theta_q$ are the model parameters, and q is the order of the moving average.

The accuracy of ARIMA predictions hinges on the orders p and q. Traditionally, the Akaike Information Criterion (AIC) is employed to determine these values. We provide ARIMA (p, m, q) with a time-based SNR sequence $(\gamma_{k-l}, \gamma_{k-l+1}, ..., \gamma_k)$ of length l and systematically explore parameters p and q. ARIMA generates a series of n-step forecast values $(\hat{\gamma}_{k-n}, \hat{\gamma}_{k-n+1}, ..., \hat{\gamma}_k)$. By subtracting the predicted SNR values from the actual SNR, we derive a series of residual errors $(e_{k-n+1}, e_{k-n+2}, ..., e_k)$. Subsequently, we feed this residual sequence into BiLSTM.

BiLSTM extends the concept of LSTM by combining two LSTM layers: one processes the forward direction of time-series data, and the other handles the reverse direction [15]. The outputs from each direction are then concatenated. This bidirectional structure allows the network to simultaneously obtain contextual information from both past and future. The algorithmic flow of a forward LSTM layer is as follows:

$$f_t = \sigma(W_f[h_{t-1}^{'}, e_{t-1}] + b_f), \tag{18}$$

$$i_t = \sigma(W_i[h_{t-1}^{'}, e_{t-1}] + b_i), \tag{19}$$

$$\tilde{C}_t = \tanh(W_C[h_{t-1}^{'}, e_{t-1}] + b_c), \tag{20}$$

$$C_t = f_t \cdot C_{t-1} + i_t \cdot \tilde{C}_t, \tag{21}$$

$$e_t = \sigma(W_o[h_{t-1}^{'}, e_{t-1}] + b_o), \tag{22}$$

$$h_t^{'} = e_t \cdot \tanh(C_t). \tag{23}$$

The six equations above describe the computations for the forget gate, input gate, candidate cell state, updated cell state, output gate, and hidden state update in an LSTM neural network. Where W represents the weight matrices, b denotes the bias vectors, σ is the sigmoid activation function and e is the residual error as the input.

Let $e_t^{''}$ be the output of the backward LSTM layer, then the final output of the BiLSTM is the concatenation of the forward and backward outputs:

$$e_t = [e_t^{'}, e_t^{''}]. \tag{24}$$

The output of the BiLSTM is the prediction of the residual error for the next time step. Our goal is to find the p_k and q_k values that minimize the residual error. Finally, these two orders are set as inputs to ARIMA, with the output being the predicted value at time $k+n$:

$$\hat{\gamma}_{k+n} = \mu + \sum_{i=1}^{p_k} \phi_i \Delta^d \gamma_{k-i} + \alpha_k + \sum_{j=1}^{q_k} \theta_j \alpha_{k-j}. \tag{25}$$

One notable limitation of the ARIMA algorithm is its inherent tendency to capture linear relationships exclusively. Given the heightened susceptibility of higher-order modulation schemes to nonlinear distortion, it becomes imperative to evaluate the ramifications of this factor. The BiLSTM algorithm can avoid long-term dependency issues through deliberate design, and its network structure is flexible, allowing for the

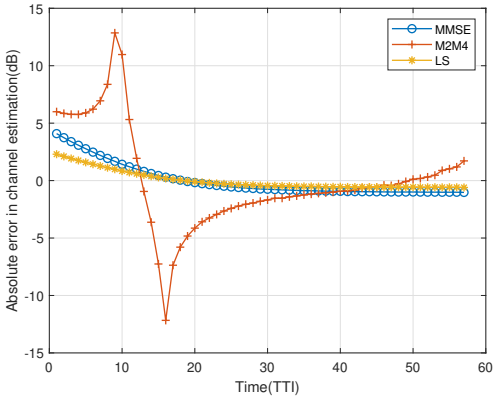

Fig. 3. Absolute error comparison of various channel state estimation algorithms.

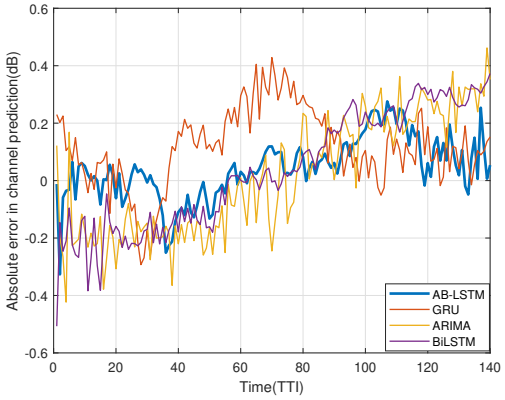

Fig. 4. Absolute error comparison of various channel state prediction algorithms.

exploration of implicit nonlinear relationships in the data. Therefore, the algorithm combining ARIMA and BiLSTM holds promise for improving the accuracy of channel state prediction. See Algorithm 1 for the algorithm flow.

C. MCS Switching Strategy

We adopt a fixed threshold switching strategy. First, we select the 42 MCSs defined in the DVB-S2X standard for simulation and obtain their SNR-BER curves. Then, we set the BER at the switching point to 10^{-3} and obtain the SNR threshold values for these 42 MCSs.

IV. Numerical Simulations

In this section, we use the previously established channel model to calculate the total loss variation within the satellite's communication range and input the loss into the DVB-S2X system. We assess the ACM method's performance with LS and AB-LSTM algorithms using simulation parameters from TABLE I. Fig. 3 presents a comparison of the performance of the LS estimator we used with two other estimation algorithms, minimum mean square error (MMSE) and second and fourth order moments (M2M4). The input SNR ranges from -10 to 26 dB in increments of 0.47 dB. Among these, the M2M4 estimator is a channel estimator based on statistical moments and is a non-data-aided (NDA) estimation method. However, both the LS and MMSE estimators are data-aided (DA) estimation methods, which results in their superior estimation accuracy. Due to the LS estimator's more effective handling of the signal's time-varying nature, the performance of the LS estimator is better than that of the MMSE estimator.

TABLE I
SIMULATION PARAMETERS

Parameters	Value
Height of the LEO satellite	680 km
Location of the ground station	$39.9°N, 116.4°E$
Carrier Frequency	30 GHz
Encoder	LDPC and BCH
Modulation order of APSK	8,16,32,64,128,256
Data frame length	64800 bit
Roll-off factor of raised cosine filter	0.35

Fig. 4 presents a comparative analysis of our proposed AB-LSTM algorithm against three benchmark algorithms: ARIMA, BiLSTM, and gated recurrent unit (GRU). The comparison focuses on the absolute errors generated by each of the four forecasting algorithms. It can be observed that the predictive performance of GRU is slightly inferior to other algorithms due to our limited training data. As analyzed in the previous section, the predictions from ARIMA exhibit significant fluctuations. BiLSTM follows the same prediction trend as ARIMA but with less volatility in its predicted values. AB-LSTM clearly compensates for the shortcomings of BiLSTM and ARIMA, achieving better forecasting performance. As can be more evidently seen from TABLE II, compared to the other three algorithms, AB-LSTM exhibits lower mean squared error (MSE), root mean squared error (RMSE), and mean absolute error (MAE).

TABLE II
PERFROMANCE OF PREDICTION ALGORITHMS

Prediction ALGORITHMS	MSE	RMSE	MAE
GRU	0.0436	0.2089	0.1868
ARIMA	0.0429	0.2071	0.1781
BiLSTM	0.0321	0.1792	0.1492
AB-LSTM	0.0132	0.1148	0.0883

Fig. 5 illustrates the SNR trends within the communicable range of our selected satellite and the process of CQI index switching in the ACM strategy. Based on our selected communication parameters, the SNR range input into the DVB-S2X is [13.12, 24.05] dB. The transmitter performs MCS switching based on CQI indications, with the CQI index range used being [17, 42]. It can be observed that the trend of CQI index switching corresponds with the trend of SNR changes, and the transmitter's MCS has been correctly switched in accordance with the variations in SNR.

Fig. 6 provides a detailed illustration of the ACM strategy applied to the DVB-S2X system. Within the specified SNR

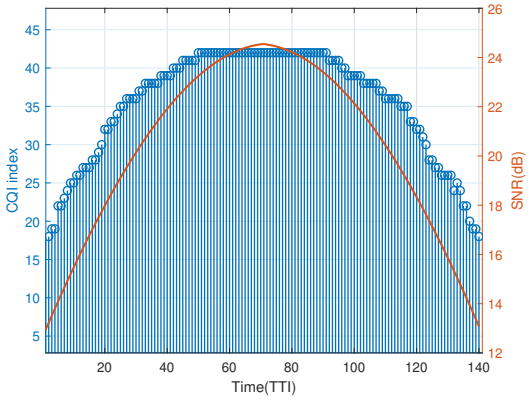

Fig. 5. Channel SNR variations and the corresponding CQI indices used.

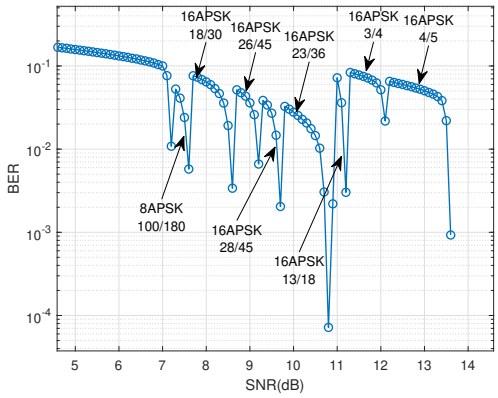

Fig. 6. ACM method in DVB-S2X.

range, the transmitter performs real-time switching of the MCS. When the SNR reaches 7.2 dB, the MCS switches to '8APSK 100/180', when the SNR reaches 7.5 dB, the MCS switches to '16APSK 18/30'. As the channel condition improves, the MCS will switch to higher-order modulation schemes or higher code rates, fully utilizing the channel capacity. It can be observed that ACM has optimized the selection method for MCS, reducing the system's complexity while meeting the BER requirements.

V. Conclusion

In this paper, we have investigated the ACM method under the DVB-S2X physical layer standard. Specifically, we have established a more realistic channel model that closely aligns with actual conditions, taking into account multiple fading factors. We have proposed an LS algorithm for channel state estimation, followed by the introduction of an AB-LSTM algorithm for channel state prediction. Based on the predicted SNR values, we have consulted a threshold table to perform MCS switching. Numerical results have shown that our proposed algorithm can achieve better estimation and prediction performance and the ACM method can accurately perform MCS switching, effectively enhancing the system's reliability and stability in LSTN scenarios characterized by high latency. In the future, we will explore more efficient and accurate ACM methods based on ultra-dense LSTN communication scenarios.

Acknowledgement

This work was supported in part by the National Key R&D Program of China under Grant 2020YFB1806104, in part by the Natural Science Fund for Distinguished Young Scholars of Jiangsu Province under Grant BK20220067, in part by the National Natural Science Foundation Original Exploration Project of China under Grant 62250004, in part by the National Natural Science Foundation of China under Grant 62271244.

References

[1] T. Ma, B. Qian, X. Qin, X. Liu, H. Zhou, and L. Zhao, "Satellite-terrestrial integrated 6G: An ultra-dense LEO networking management architecture," *IEEE Wireless Communications*, vol. 31, no. 1, pp. 62–69, 2024.

[2] X. Zhang, B. Qian, X. Qin, T. Ma, J. Chen, H. Zhou, and X. S. Shen, "Cybertwin-assisted mode selection in ultra-dense LEO integrated satellite-terrestrial network," *Journal of Communications and Information Networks*, vol. 7, no. 4, pp. 360–374, 2022.

[3] J. Xue, K. Yu, T. Zhang, H. Zhou, L. Zhao, and X. Shen, "Cooperative deep reinforcement learning enabled power allocation for packet duplication urllc in multi-connectivity vehicular networks," *IEEE Transactions on Mobile Computing*, pp. 1–15, 2024.

[4] X. Liu, T. Ma, Z. Tang, X. Qin, H. Zhou, and X. S. Shen, "Ultrastar: A lightweight simulator of ultra-dense LEO satellite constellation networking for 6G," *IEEE/CAA Journal of Automatica Sinica*, vol. 10, no. 3, pp. 632–645, 2023.

[5] F. M. Alawwad, Y. A. Al-Zahrani, and H. M. Behairy, "Maximizing system capacity using adaptive coding and modulation techniques for slowly fading channels," in *2017 UKSim-AMSS 19th International Conference on Computer Modelling & Simulation (UKSim)*, 2017, pp. 221–226.

[6] C. Xu, F. Liu, J. Yang, Z. Xiao, and Z. Han, "A sparse bayesian learning method of joint activity detection and channel estimation for LEO grant-free random access," in *2023 IEEE 24th International Workshop on Signal Processing Advances in Wireless Communications (SPAWC)*, 2023, pp. 391–395.

[7] Y. Ji, G. Zhang, J. Huang, J. Yang, G. Gui, and H. Sari, "Deep learning for adaptive modulation and coding with payload length in vehicle-to-vehicle communications systems," in *2021 IEEE 94th Vehicular Technology Conference (VTC2021-Fall)*, 2021, pp. 1–5.

[8] R. Guo, K. Wang, Z. Deng, W. Lin, and R. Song, "A prediction model for channel state information in satellite communication system," in *2020 IEEE 31st Annual International Symposium on Personal, Indoor and Mobile Radio Communications*, 2020, pp. 1–6.

[9] B. Chen, Y. Lei, D. Lavery, C. Okonkwo, and A. Alvarado, "Rate-adaptive coded modulation with geometrically-shaped constellations," in *2018 Asia Communications and Photonics Conference (ACP)*, 2018, pp. 1–3.

[10] ETSI, "Second generation framing structure, channel coding and modulation systems for broadcasting, interactive services, news gathering and other broadband satellite applications; part 2: DVB-S2 extensions (DVB-S2X)," European Telecommunications Standards Institute (ETSI), Standard EN 302 307-2 V1.3.1, July 2021.

[11] International Telecommunication Union, "Prediction of clutter loss," ITU-R Recommendation, Tech. Rep. ITU-R P.2108-1, 2021.

[12] International Telecommunication Union, "Propagation data and prediction methods required for the design of earth-space telecommunication systems," ITU-R Recommendation, Tech. Rep. ITU-R P.618-14, 2023.

[13] International Telecommunication Union, "Attenuation due to clouds and fog," ITU-R Recommendation, Tech. Rep. ITU-R P.840-9, 2023.

[14] International Telecommunication Union, "Attenuation by atmospheric gases," ITU-R Recommendation, Tech. Rep. ITU-R P.676-6, 2005.

[15] X. Zhou, A. Pranolo, and Y. Mao, "AB-LSTM: Attention bidirectional long short-term memory for multivariate time-series forecasting," in *2023 International Conference on Computer, Electronics & Electrical Engineering & their Applications (IC2E3)*, 2023, pp. 1–6.